Quantum Calculation of Molecular Energies and Energy Gradients in Solution by a Conductor Solvent Model

Vincenzo Barone and Maurizio Cossi*

Dipartimento di Chimica, Università Federico II, via Mezzocannone 4, I-80134 Napoli, Italy

Received: May 21, 1997; In Final Form: October 17, 1997

A new implementation of the conductor-like screening solvation model (COSMO) in the GAUSSIAN94 package is presented. It allows Hartree−Fock (HF), density functional (DF) and post-HF energy, and HF and DF gradient calculations: the cavities are modeled on the molecular shape, using recently optimized parameters, and both electrostatic and nonelectrostatic contributions to energies and gradients are considered. The calculated solvation energies for 19 neutral molecules in water are found in very good agreement with experimental data; the solvent-induced geometry relaxation is studied for some closed and open shell molecules, at HF and DF levels. The computational times are very satisfying: the self-consistent energy evaluation needs a time 15−30% longer than the corresponding procedure in vacuo, whereas the calculation of energy gradients is only 25% longer than in vacuo for medium size molecules.

1. Introduction

Many chemical reactions of biological and technological relevance take place in a condensed medium, in particular in liquid solutions, and often an accurate theoretical treatment of such processes cannot leave a realistic description of the environmental effects aside. The recent advances in quantum calculation techniques are making ab initio calculations possible on systems of ever-increasing size: thus there is a growing need of ab initio procedures providing reliable treatments of solute−solvent interactions.

Among the several approaches proposed to describe the solvent effect at the ab initio level, continuum models are quite popular,[1−4] due to their flexibility and efficiency. In such models the solute molecule, possibly supplemented by some solvent molecules belonging to the first solvation shell, is placed in a cavity surrounded by a polarizable continuum, whose reaction field modifies the energy and the properties of the solute. In the most advanced ab initio models (e.g., PCM,[5,6] SCIPCM,[7] SCRF,[8,9] COSMO,[10,11] and GCOSMO[12]) the cavities are of molecular shape, and the reaction field is described in terms of apparent polarization charges or reaction field factors included in the solute Hamiltonian, so that it is possible to perform iterative procedures leading to the self-consistence between the solute wave function and the solvent polarization. Quantum calculations considering the solvent reaction field are not limited to monodeterminant wave functions: for example, Mikkelsen et al.[13,14] and Karlström[15] have proposed multiconfigurational procedures where the solvent is described by a continuum dielectric.

In addition, some models also describe nonelectrostatic solute−solvent interactions (which are usually referred to as cavitation, dispersion, and repulsion energies). Moreover, the geometry relaxation induced by the solvent on the solute molecules cannot often be neglected; thus an efficient solvation model must provide energy gradients and allow geometry optimizations in solution. In other words, it is desirable that both direct (i.e., polarization) and indirect (i.e., relaxation) solvent effects are treated with the same accuracy.

In this work we report the novel implementation in the package GAUSSIAN94[16] of an ab initio solvation model based on the conductor-like solvation model (COSMO), first proposed by Klamt and Schüürmann for classical calculations[10] and then extended to quantum mechanical systems.[11,12] The present implementation allows Hartree−Fock (HF), density functional (DF), and post-HF energy calculations and HF and DF geometry optimizations in solution; moreover, all the manipulations of the molecular wave function provided by GAUSSIAN94 for isolated systems are available for solvated molecules also.

The COSMO approach describes the solvent reaction field by means of apparent polarization charges distributed on the cavity surface, which are determined by imposing that the total electrostatic potential cancels out on the surface. This boundary condition, suited for cavities in conductor media, can describe (i) the interaction between molecules and metals (e.g., in the simulation of electrodic processes) and (ii) the solvation in polar liquids.

For the latter applications, the conductor-like model is physically less founded than dielectric models; nevertheless, the conductor approach is attractive, since its boundary condition is computationally simpler, especially in the expression of the energy gradients. Some authors have pointed out that the conductor model well reproduces the solute energies and properties obtained with the dielectric approach, using the dielectric constants characteristic of polar solvents.[12,17] Our results confirm that, using cavity parameters optimized for the well-known polarizable continuum model (PCM), the COSMO procedure gives hydration energies in very good agreement with the experimental results.

The present implementation also provides the nonelectrostatic contributions to the solute free energy and the first derivatives of these contributions with respect to the nuclear coordinates: some examples of geometry optimizations are reported, using both the electrostatic and the nonelectrostatic terms. To our knowledge, these are the first examples of complete geometry optimizations for a conductor model. In fact the derivatives of the nonelectrostatic solute−solvent energies require an accurate description of the changes induced on the cavity shape by the nuclear motion, which is provided by a recently developed procedure.[18] On the other hand, the electrostatic energy gradients also are improved by considering these geometrical contributions properly.

S1089-5639(97)01699-X CCC: $15.00
Published on Web 02/20/1998

2. Theoretical Background

2.1. Definition of the Cavity. The solute molecules are embedded in cavities formed by interlocking spheres centered on the solute atoms or atomic groups. The surface is smoothed by adding some other spheres, not centered on atoms, to simulate the so-called solvent-excluding surface, following the GEPOL procedure.[19−21] Then, the cavity surface is partitioned into small domains, called tesserae, obtained by projecting on the surface the faces of polyhedra inscribed in each sphere; the tesserae completely buried into other spheres are discarded, and those partially cut are replaced by suitable polygons.[18]

The present implementation exploits the recently developed PolyGen procedure,[22,23] allowing a wide choice of polyhedra, so that the surface can be covered with finer and finer tessellations, if needed. A long experience with PCM calculations indicates that a tessellation using 60 tesserae per sphere (obtained by projecting the faces of inscribed pentakisdodecahedra) is a reasonable compromise between accuracy and efficiency; we shall show that this tessellation can be used in standard COSMO calculations, too. Anyway, it is a good rule to verify the invariance of the results with respect to this parameter, at least in test cases.

2.2. Molecular Free Energy. Under the influence of the solvent, the molecular Hamiltonian is perturbed:

$$\hat{H} = \hat{H}^0 + \hat{V} \tag{1}$$

where $\hat{H}^0$ is the Hamiltonian of the isolated solute; the operator $\hat{V}$, describing the electrostatic solute−solvent interactions, linearly depends on the solute wave function $|\Psi\rangle$: in this case, it has been shown[24] that the SCF procedure leads to the variational minimization of the free energy of the solute, G:

$$G = \langle\Psi|\hat{H}^0|\Psi\rangle + \frac{1}{2}\langle\Psi|\hat{V}|\Psi\rangle \tag{2}$$

The interaction operator $\hat{V}$ is written in terms of apparent polarization charges: in each tessera i a charge q_i appears, according to the conductor-like boundary condition:

$$V(\vec{r}) + \sum_i^{\text{tesserae}} V_{q_i}(\vec{r}) = 0 \tag{3}$$

where V and V_{q_i} are the electrostatic potential due to the solute and to the polarization charges, respectively, and $\vec{r}$ is a point on the surface. The vector of the conductor-like polarization charges, **Q**, can be determined by the equation

$$\mathbf{AQ} = -\mathbf{V} \tag{4}$$

where the vector **V** contains the electrostatic potential due to the solute on the tesserae. The elements of the matrix **A** are

$$A_{ii} = 1.07\sqrt{\frac{4\pi}{S_i}} \tag{5}$$

$$A_{ij} = \frac{1}{|\vec{r}_i - \vec{r}_j|} \tag{6}$$

where S_i is the area of tessera i; the expression for A_{ii} has been found by Klamt and Schüürmann in the case of a single sphere partitioned into a variable number of identical tesserae[10] and also used by Truong and Stefanovich in their own GCOSMO implementation.[12]

If the COSMO model is used to simulate a solvent with dielectric constant ϵ, the polarization charges have to be scaled so that the total polarization charge will obey the Gauss law: a very effective way to do this is multiplying each charge by the factor $(\epsilon-1)/\epsilon$, so that the actual charges are

$$\mathbf{q} = \frac{\epsilon - 1}{\epsilon}\mathbf{Q} \tag{7}$$

In analogy with the boundary element method formulation of PCM,[24] it is convenient to separate the potential due to the solute nuclei, V^N, and that due to the electrons, V^e, defining two sets of charges:

$$\mathbf{AQ}^N = -\mathbf{V}^N; \quad \mathbf{q}^N = \frac{\epsilon - 1}{\epsilon}\mathbf{Q}^N \tag{8}$$

$$\mathbf{AQ}^e = -\mathbf{V}^e; \quad \mathbf{q}^e = \frac{\epsilon - 1}{\epsilon}\mathbf{Q}^e \tag{9}$$

In a finite basis matrix formulation, the molecular Hamiltonian in the presence of the solvent can be written

$$\mathbf{H} = \mathbf{H}^0 + \frac{1}{2}(\mathbf{j} + \mathbf{y}) + \frac{1}{2}\mathbf{X} + \frac{1}{2}U_{NN} \tag{10}$$

where

$$\mathbf{H}^0 = \mathbf{h}^0 + \frac{1}{2}\mathbf{G}^0 + V_{NN} \tag{11}$$

is the Hamiltonian for the isolated molecule, and **j**, **y**, **X**, and U_{NN} represent the interactions between $\mathbf{q}^e$ and the solute nuclei, $\mathbf{q}^N$ and the solute electrons, $\mathbf{q}^e$ and the electrons, and $\mathbf{q}^N$ and the nuclei, respectively. The explicit expressions for these terms have been presented elsewhere for the PCM model;[6] they can be used in this framework without changes.

The corresponding Fock matrix is

$$\mathbf{F} = \mathbf{F}^0 + \frac{1}{2}(\mathbf{j} + \mathbf{y}) + \mathbf{X} \tag{12}$$

$$\mathbf{F}^0 = \mathbf{h}^0 + \mathbf{G}^0 \tag{13}$$

In these terms it is possible to perform an iterative calculation, formally equal to the usual SCF procedure for isolated molecules, leading to self-consistent polarization charges and solute wave function. Notice that both Hartree−Fock and density functional, as well as hybrid HF−DF, Hamiltonians can be modified according to eq 10. Moreover, the present implementation allows us to perform perturbative many-body (MPn), configuration interaction, and coupled cluster calculations using the polarization charges determined at the HF level or iterating the calculation to get a complete self-consistence between the polarization charges and the post-Hartree−Fock wave function, following the same procedure illustrated for the PCM method, e.g., in ref 25.

The total polarization charges appearing on the cavity surface are subject to Gauss' law:

$$\sum_i q_i^N = q_{\text{Gauss}}^N = -\frac{\epsilon - 1}{\epsilon}\sum_n^{\text{nuclei}} Z_n \tag{14}$$

$$\sum_i q_i^e = q_{\text{Gauss}}^e = \frac{\epsilon - 1}{\epsilon}N^e \tag{15}$$

where Z_n and N^e are the atomic number of nucleus n and the

number of solute electrons, respectively. In practice, the conditions 14 and 15 are not fulfilled, both for numerical and for physical reasons: the numerical error arises from the approximated description of the polarization charge density in terms of discrete point charges; the physical error is due to the little amount of solute charge escaping from the cavity because of the exponential decay of the electronic tails. The numerical error is present for both $\mathbf{q}^N$ and $\mathbf{q}^e$, approximately at the same extent, whereas the escaped charge error, usually heavier than the former one, affects $\mathbf{q}^e$ only. Some methods have been proposed to correct such effects, both in dielectric[26] and in conductor models;[27] however, it is known that the conductor approach is less sensitive to these sources of error than the dielectric one, and actually we found that the calculated COSMO charges for neutral solutes sensibly satisfy eqs 14 and 15 (see below). Then we deferred the treatment of numerical and electronic errors to a further work, devoted to ionic solutes.

According to eq 2 the molecular free energy in solution can be written

$$G_{es} = \langle\Psi|\hat{H}^0|\Psi\rangle + \Delta G_{es} \tag{16}$$

$$\Delta G_{es} = \frac{1}{2}\sum_i^{\text{tesserae}} (q_i^e + q_i^N)(V_i^e + V_i^N) = \frac{1}{2}\sum_i^{\text{tesserae}} q_i V_i \tag{17}$$

where the subscript "es" recalls that we are considering electrostatic interactions only: for brevity, V_i indicates the value of the electrostatic potential on the tessera i.

Recalling eqs 4 and 7, the solute potential at tessera i can be related to the set of polarization charges

$$V_i = -\frac{\epsilon}{\epsilon - 1}\sum_j^{\text{tesserae}} A_{ij} q_j \tag{18}$$

and ΔG_{es} can be put in an equivalent form,

$$\Delta G_{es} = \sum_i q_i V_i + \frac{1}{2}\frac{\epsilon}{\epsilon - 1}\sum_{ij} A_{ij} q_i q_j \tag{19}$$

that will be useful in the formulation of energy gradients.

Taking into account the nonelectrostatic interactions, the solute free energy becomes

$$G = G_{es} + G_{cav} + G_{dis} + G_{rep} \tag{20}$$

The free energy associated with the formation of the cavity in the continuum medium, G_{cav}, is calculated with the expression derived by Pierotti from the hard sphere theory,[28] adapted to the case of nonspherical cavities.[25] The dispersion and repulsion terms, G_{dis}, G_{rep}, are calculated following Floris and Tomasi's procedure,[29,30] with the parameters proposed by Caillet and Claverie;[31] the implementation details are described in ref 18. Clearly the nonelectrostatic terms are exactly the same in the PCM and the COSMO models, provided equal cavities are employed.

2.3. Free Energy Derivatives. The free energy derivatives can be written

$$G^\alpha = G_{es}^\alpha + G_{cav}^\alpha + G_{dis}^\alpha + G_{rep}^\alpha \tag{21}$$

where the superscript α indicates the partial derivative with respect to the nuclear coordinate α.

The expressions for the derivatives of the nonelectrostatic terms have been given elsewhere;[18,32] as said in the Introduction, they heavily depend on the derivatives of the tesserae geometrical elements (area, position of the vertices), which are neglected, totally or in part, in the preceding COSMO implementations.[10,11,33]

The derivative of the electrostatic contribution is

$$G_{es}^\alpha = [\langle\Psi|\hat{H}^0|\Psi\rangle]^\alpha + \Delta G_{es}^\alpha \tag{22}$$

$[\langle\Psi|\hat{H}^0|\Psi\rangle]^\alpha$ is the usual energy derivative calculated by standard programs; from eq 19 we have

$$\Delta G_{es}^\alpha = \sum_i q_i V_i^\alpha + \sum_i q_i^\alpha V_i + \frac{1}{2}\frac{\epsilon}{\epsilon - 1}\sum_{ij} A_{ij}^\alpha q_i q_j + \frac{\epsilon}{\epsilon - 1}\sum_{ij} A_{ij} q_j q_i^\alpha \tag{23}$$

Recalling eq 18, the terms depending on the derivatives of the polarization charges cancel out, leaving

$$\Delta G_{es}^\alpha = \sum_i q_i V_i^\alpha + \frac{1}{2}\frac{\epsilon}{\epsilon - 1}\sum_{ij} A_{ij}^\alpha q_i q_j \tag{24}$$

This expression for ΔG_{es}^α is computationally very efficient, since it doesn't require the calculation of charge derivatives: notice that in dielectric models an analogous expression does not exist.

The free energy derivatives (eq 21) can be used in standard optimization procedures (e.g., the Berny algorithm implemented in GAUSSIAN94, used throughout this work), in order to calculate the solvent-induced molecular relaxation.

3. Computational Details

The calculations were performed at the HF, MP2, and density functional levels; for the latter we resorted to the hybrid B3LYP functional, which combines HF and Becke[34] exchange terms with the Lee−Yang−Parr correlation functional;[35] the 6-31G(d) and 6-311+G(d,p) basis sets were used.

The solvent was water at 25 °C, with dielectric constant $\epsilon = 78.4$.

The molecular cavities were built following the UAHF (united atom for Hartree−Fock) procedure,[36] recently developed by our group for the PCM program. For the sake of clarity, we briefly resume the UAHF rules for the molecules considered in the present paper.

(1) Hydrogens don't have individual spheres; they are included in the same sphere of the heavy atom they are bonded to.

(2) The second-row atoms radii, R(X)'s, depend on the molecular environment according to

$$R(\text{X}) = 1.5\ (\text{Å}) + \gamma(n_H + 0.5\, n_{act} + \delta_{sp^2} + 1.5\delta_{sp}) \tag{25}$$

where $\gamma = 0.18$ Å for carbon and 0.09 Å for the other atoms; n_H is the number of bonded hydrogens, n_{act} is the number of bonded "active" atoms ("active" means having the same atomic number and the same hybridization state as X), and δ_{sp^2} is 1 if X is in the sp^2 hybridization state and 0 otherwise, and analogously for δ_{sp}.

(3) A further correction based on the number of substituents is applied to sp^3 carbons:

$$R(\text{C}_{sp^3}) = R(\text{C}) - 0.09(n_{\text{C}_{sp^2}} + n_O + 2n_N + n_{CX}) \tag{26}$$

where CX indicates a substituted sp^3 carbon.

TABLE 1: Experimental and COSMO Solvation Free Energies (kcal/mol). HF Calculations Have Been Repeated with Different Tessellations of the Cavity Surface; Basis Set 6-31G(d), Unless Otherwise Noted

		HF				MP2	B3LYP
tesserae per sphere:	expt	60	180	360	60[a]	60	60
CH_4	2.0	1.86	1.85	1.85	1.84	1.85	1.86
CH_3CH_3	1.8	1.96	1.95	1.95	1.93	1.95	1.96
H_2O	−6.3	−6.26	−6.30	−6.27	−6.68	−6.10	−5.53
CH_3OH	−5.1	−5.04	−5.15	−5.14	−5.52	−4.82	−4.36
CH_3OCH_3	−1.9	−2.13	−2.16	−2.16	−2.54	−1.85	−1.53
n-C_4H_9OH	−4.7	−4.46	−4.56	−4.55	−4.97	−4.23	−3.78
CH_2OH-CH_2OH	−9.6	−9.91	−9.99	−9.95	−10.76	−9.09	−8.57
NH_3	−4.3	−4.32	−4.35	−4.34	−4.49	−4.32	−3.98
CH_3NH_2	−4.6	−4.68	−4.81	−4.79	−4.98	−4.67	−4.31
$(CH_3)_2NH$	−4.3	−4.33	−4.41	−4.41	−4.76	−4.30	−3.94
$(CH_3)_3N$	−3.2	−2.79	−2.86	−2.88	−3.15	−2.74	−2.40
H_2CO	−1.7	−1.75	−1.77	−1.76	−2.36	−0.41	−0.44
CH_3CHO	−3.5	−3.53	−3.56	−3.56	−4.31	−2.00	−2.17
CH_3COCH_3	−3.8	−3.65	−3.71	−3.70	−4.47	−2.26	−2.49
HCN	−3.2	−3.07	−3.07	−3.06	−3.30	−2.15	−2.05
CH_3CN	−3.9	−3.63	−3.66	−3.65	−4.05	−2.77	−2.92
CH_3COOH	−6.7	−7.01	−7.02	−7.02	−7.77	−5.85	−5.75
CH_3COOCH_3	−3.3	−3.44	−3.49	−3.46	−3.97	−2.38	−2.43
CH_3CONH_2	−9.7	−9.33	−9.47	−9.42	−10.34	−7.90	−7.78
mean unsigned error		0.17	0.17	0.17	0.46	0.65	0.82
max error		0.41	0.39	0.35	1.16	1.80	1.83

[a] Basis set 6-311+G(d,p).

TABLE 2: Errors on Nuclear and Electronic Total Polarization Charges with Respect to Gauss' Law. Calculations at the HF/6-31G(d) Level with 60 Tesserae per Sphere

	error on nuclear charge	error on electronic charge		error on nuclear charge	error on electronic charge
CH_4	0.0009	0.0030	$(CH_3)_3N$	0.0110	0.0251
CH_3CH_3	0.0163	0.0188	H_2CO	0.0169	0.0193
H_2O	0.0008	0.0028	CH_3CHO	0.0081	0.0133
CH_3OH	0.0077	0.0129	CH_3COCH_3	0.0297	0.0356
CH_3OCH_3	0.0062	0.0123	HCN	0.0130	0.0154
n-C_4H_9OH	0.0399	0.0473	CH_3CN	0.0134	0.0173
CH_2OH-CH_2OH	0.0233	0.0355	CH_3COOH	0.0099	0.0148
NH_3	0.0010	0.0052	CH_3COOCH_3	0.0127	0.0188
CH_3NH_2	0.0099	0.0199	CH_3CONH_2	0.0135	0.0197
$(CH_3)_2NH$	0.0035	0.0162			

The above rules have been coded in a routine implemented in GAUSSIAN94[36] that automatically assigns the proper atomic and group radii. The UAHF cavities allow one to calculate PCM solvation energies at the HF level in excellent agreement with the experimental results; we shall show that they are suitable for COSMO calculations, too.

4. Results and Discussion

In Table 1 we report the experimental and calculated solvation free energies for 19 neutral molecules; the calculations have been performed with the COSMO model at the HF, MP2, and B3LYP levels. The MP2 energies have been obtained using the polarization charges determined at the HF level; this procedure gives a good approximation of the completely self-consistent calculation in the solvent.[38]

The good agreement between HF/6-31G(d) and experimental energies clearly shows that the UAHF cavity model, though developed for PCM calculations, can be satisfactorily used in the COSMO framework, too. We recall however that in the present implementation other commonly used atomic radii sets (e.g., Pauling's[39] and Bondi's[40] ones) can be selected by simply assigning a keyword the proper value. MP2 and B3LYP results listed in Table 1 are less accurate than HF ones, although the mean errors are quite small in any case. In fact it is well-known that correlated methods usually yield smaller calculated dipole moments, and since the size of the cavities is optimized for HF wave functions, the solvent reaction field is underestimated at the MP2 and DF levels: suitable united atom cavity models for DF and post-HF calculations are in preparation. On the other hand, both dipole moments and polarizabilities are usually larger when calculated with extended basis sets, and solvation energies are overestimated at the HF/6-311+G(d,p) level, although the errors remain small.

The magnitude of the numerical error, due to the discretization of the polarization charge density in a finite number of point charges, can be reduced by increasing the number of surface tesserae. In Table 1 we report COSMO solvation energies calculated at the HF level with different surface tessellations: it is apparent that the results are remarkably stable with respect to this parameter, so that the default value of 60 tesserae per sphere has been selected in all the calculations.

In Table 2 we report the difference between the total polarization charges induced by solute nuclei, $\sum_i q_i^N$, and by electrons, $\sum_i q_i^e$, and the values predicted by Gauss law, eqs 14 and 15, recalling that the discrepancy between $\sum q_i^N$ and q_{Gauss}^N is another measure of the discretization error, whereas the disagreement between $\sum q_i^e$ and q_{Gauss}^e depends both on the discretization and on the error due to the electronic tails escaped from the cavity.

The results listed in Table 2 confirm that the discretization error is very small, and show that the electronic error too is not

TABLE 3: Optimized Geometry (Bond Lengths in Å, Angles in deg), Dipole Moment (D), and Free Energies (hartrees) in Vacuo and in Solution for Two Acetic Acid Conformers (See Figure 2) Calculated at the B3LYP Level with the 6-31G(d) and 6-311+G(d,p) Basis Sets

	syn conformer				anti conformer			
	6-31G(d)		6-311+G(d,p)		6-31G(d)		6-311+G(d,p)	
	in vacuo	in water (COSMO)	in vacuo	in water (COSMO)	in vacuo	in water (COSMO)	in vacuo	in water (COSMO)
R(C−C)	1.509	1.504	1.504	1.498	1.520	1.517	1.516	1.508
R(C−H_t)	1.090	1.091	1.088	1.089	1.090	1.092	1.087	1.089
R(C−H_g)	1.095	1.096	1.092	1.094	1.097	1.097	1.093	1.094
R(C═O)	1.210	1.215	1.205	1.213	1.203	1.218	1.196	1.208
R(C−O)	1.359	1.348	1.359	1.341	1.365	1.359	1.364	1.352
R(O−H)	0.976	0.988	0.969	0.986	0.971	0.986	0 963	0.981
∠CCH_t	106.54	109.83	109.56	110.17	109.27	109.88	109.30	109.88
∠CCH_g	110.00	110.01	109.84	109.75	110.70	110.17	110.47	110.59
∠CC═O	126.23	125.96	126.15	125.76	124.86	124.00	124.91	123.75
∠CC−O	111.35	112.03	111.53	112.63	115.20	114.59	115.31	116.64
∠COH	105.92	107.49	107.08	109.27	110.11	110.84	110.86	111.14
∠H_gCCO	121.00	120.95	121.04	121.10	120.22	120.72	120.23	120.45
dipole moment	1.58	2.03	1.74	2.34	4.30	5.90	4.57	6.06
energy	−229.081 78	−229.091 40	−229.164 72	−229.163 99	−229.071 91	−229.088 76	−229.155 30	−229.172 00

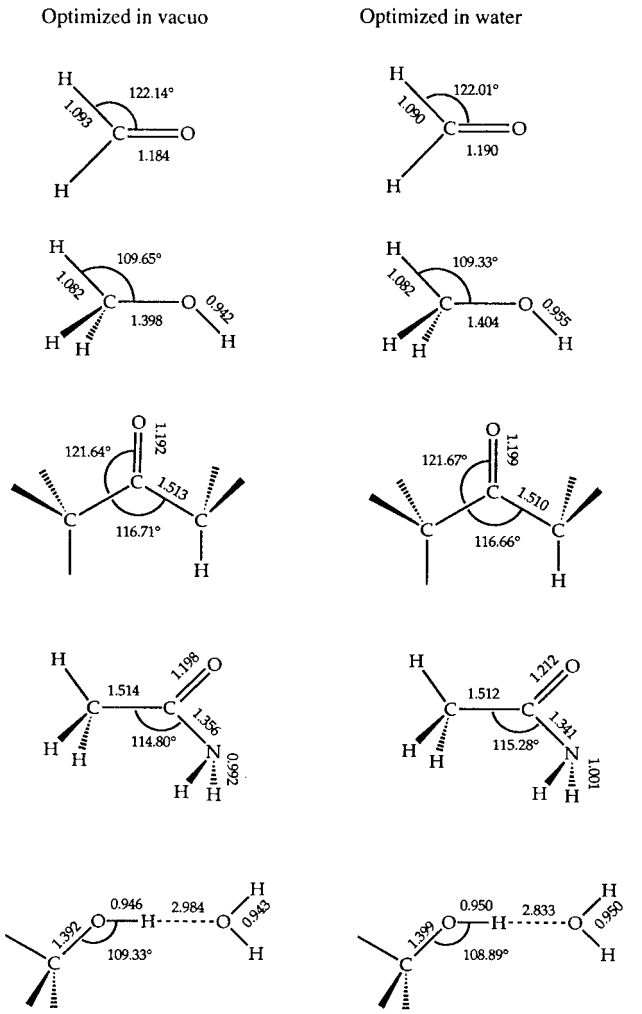

Figure 1. Geometrical parameters optimized in vacuo and in solution at the HF/6-31G(d) level for some molecules.

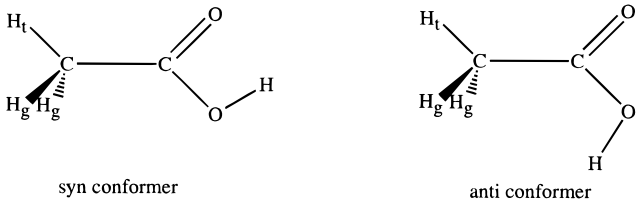

Figure 2. Acetic acid conformers.

serious for neutral solutes with this kind of cavity, thus justifying the use of $\mathbf{q}^N$ and $\mathbf{q}^e$ as derived from eqs 8 and 9, without further corrections.

The effects of the geometry reoptimization in water on some molecules at the HF level are shown in Figure l: the COSMO calculations of the free energy gradient, including the derivatives of the nonelectrostatic energies, led the optimization procedure to converge in all the presented cases without particular problems: note that the convergence thresholds were the same as in usual GAUSSIAN94 calculations for isolated molecules (convergence thresholds: 0.00045 au for the maximum force, 0.0003 au for the mean force, 0.0018 au for the maximum predicted displacement, and 0.0012 au for the mean displacement).

As one could expect, the solvent effect on the geometry relaxation becomes more important when ionic resonance structures are present (e.g., in acetamide) and in H-bonded complexes. We stress that in these geometry optimizations the

TABLE 4: Energy Differences (kcal/mol) between the Syn and Anti Acetic Acid Conformers, Calculated with the 6-311+G(d,p) Basis Set

level of the calculation	$E(syn) - E(anti)$ in vacuo	$G(syn) - G(anti)$ in water	$\Delta G_{solv}(syn) - \Delta G_{solv}(anti)$
HF[a]	6.70	2.39	−4.31
MP2[b]	6.03	2.55	−3.48
MP4[b]	5.83		
QCISD[b]	5.85		
B3LYP[c]	5.91	2.33	−3.52
B3LYP[d]		2.19	−3.72

[a] Geometries optimized in vacuo at the HF/6-311+G(d,p) level. [b] Geometries optimized in vacuo at the MP2/6-311+G(d,p) level. [c] Geometries optimized in vacuo at the B3LYP/6-311+G(d,p) level. [d] Geometries optimized in water at the B3LYP/6-311+G(d,p) level.

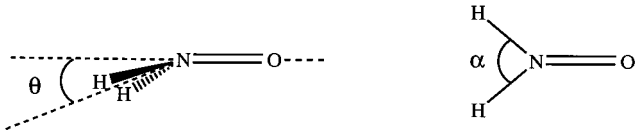

Figure 3. Bond angle and out-of-plane angle for the H_2NO radical.

TABLE 5: Equilibrium and Planar Geometries (Bond Lengths in Å, Angles in deg) Optimized in Vacuo and in Solution for H_2NO (See Figure 3) at the UB3LYP/ 6-311G(d,p) Level

	equilibrium		planar (saddle point)	
	in vacuo	in water	in vacuo	in water
R(N−H)	1.018	1.024	1.016	1.024
R(N═O)	1.277	1.279	1.275	1.279
α	59.11	59.6	59.72	59.86
θ	17.39	9.88	0.0	0.0

TABLE 6: Vibrational Frequencies (cm^{-1}) Calculated at the UB3LYP/6-311G(d,p) Level for Planar H_2NO in Vacuo and in Solution

vib mode	in vacuo	in water
a_1	3421.9	3290.5
a_1	1681.7	1655.5
a_1	1389.5	1394.7
b_2	3548.2	3425.9
b_2	1271.4	1267.6
b_1	227.0i	148.4i

expression 21 for the energy derivatives was used; for the first time, the complete derivatives of tesserae area and shape were taken into account in the COSMO framework, allowing the calculation of nonelectrostatic energy derivatives and improving the electrostatic energy derivatives, too.

Next we considered the effect of the solvation on the structures and the energy gap between the two conformers of acetic acid illustrated in Figure 2.

In Table 3 we show the effect of the reoptimization in water on the structure and the free energy of both conformers, calculated at the B3LYP/6-311G+(d,p) level; in Table 4 the energy difference between the syn and the anti conformers calculated at different levels (with 6-311G+(d,p) basis set) in vacuo and in solution is reported.

From the data in Table 3, one can see that in the isolated molecules some geometrical parameters are quite dependent on the quality of basis set, whereas such dependence is less pronounced for the solvent-induced rearrangements.

The conformational energy difference in vacuo calculated at the QCISD level is 5.85 kcal/mol, exactly as the best value previously obtained by MP3/6-311+G(d,p) calculations,[37] whereas Andzelm et al.[11] obtained 5.1 and 4.8 kcal/mol using a local density functional and a gradient-corrected (BP) functional, respectively; thus, our B3LYP result in vacuo (5.91 kcal/mol)

TABLE 7: Molecular Energies (hartrees) and Isotropic Hyperfine Coupling Constants (G) for H_2NO in Vacuo and in Solution Calculated at the UB3LYP/6-311G(d,p) Level

	equilibrium			planar		
	in vacuo	in water at the geometry optimized in vacuo	in water at the geometry optimized in water	in vacuo	in water at the geometry optimized in vacuo	in water at the geometry optimized in water
energy	−131.129 763	−131.142 477	−131.142 639	−131.129 709	−131.142 506	−131.142 658
a(N)	6.69	8.01	5.97	4.19	5.12	5.22
a(H)	−10.19	−10.13	−13.93	−13.97	−15.22	−15.20
a(O)	−11.44	−11.25	−11.23	−11.42	−11.24	−11.22

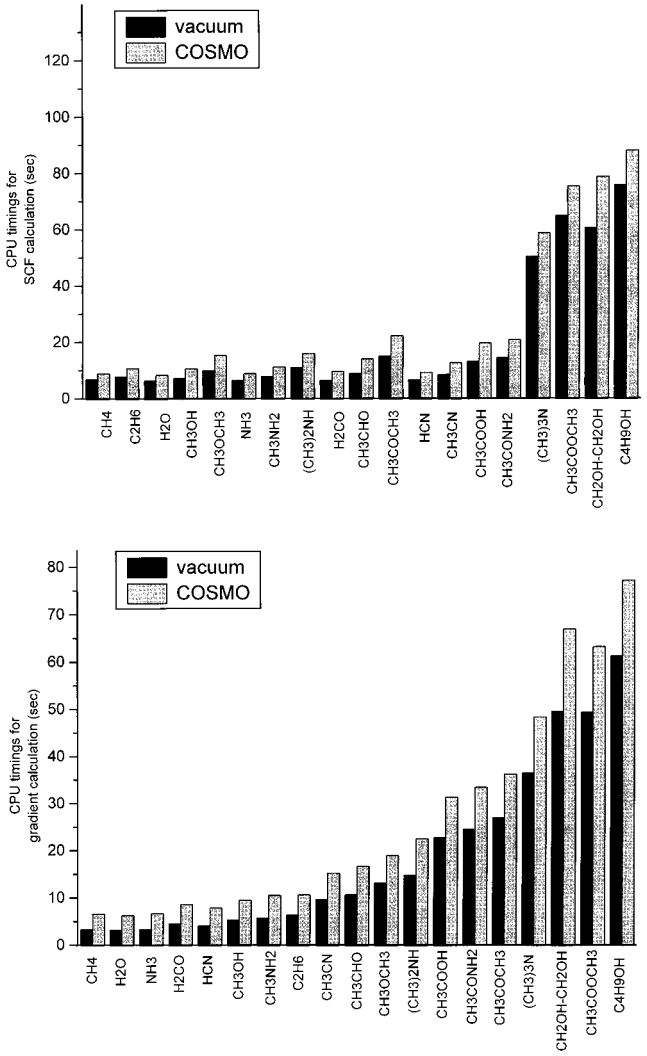

Figure 4. CPU times (on an IBM Rise 6000/560) for energy and gradient calculations in vacuo and in solution.

is quite satisfactory. At the B3LYP/6-311+G(d,p) level the syn−anti energy difference in water is 2.33 kcal/mol with the geometries optimized in vacuo and 2.19 kcal/mol after reoptimization in solution; that is, the solvent stabilizes the anti conformer with respect to the syn form by 3.72 kcal/mol. This value is in quite good agreement with the results obtained, without geometry reoptimization, by Andzelm et al.[11] with their own COSMO implementation that yielded a stabilization of 3.3 kcal/mol using their local functional and 3.1 kcal/mol using the BP functional.

To test the COSMO procedure on open shell systems, we optimized the geometry of H_2NO in vacuo and in water at the UB3LYP/6-311G(d,p) level; the results for both the equilibrium bent structure and the saddle point planar structure (see Figure 3) are summarized in Table 5. This system has been widely studied by many groups, since it is representative of a class of relatively stable radicals that have been experimentally characterized in many liquid media.

TABLE 8: Vibrational Average (at 298 K) of Out-of-Plane Angle (θ in Figure 3, in deg), hcc's (G), and Dipole Moment (D) for H_2NO in Vacuo and in Solution Calculated at the UB3LYP/6-311+G(d,p) Level

	in vacuo	in water
$(\langle\theta^2\rangle_{298})^{1/2}$	18.8	18.3
$\langle a(\mathrm{N})\rangle_{298}$	6.9	7.2
$\langle a(\mathrm{H})\rangle_{298}$	−9.8	−10.9
$\langle\mu\rangle_{298}$	3.03	3.83

Vibrational frequencies for the planar structure are reported in Table 6; we find an imaginary frequency corresponding to the out-of-plane bending of hydrogens, confirming that this structure is a saddle point both in vacuo and in solution. COSMO frequencies have been obtained numerically, since the implementation of analytic energy second derivatives in this framework is still in progress.

Then, in Table 7 we compare the solvent effects due to the direct solute polarization to the effects induced by the geometry rearrangement on the SCF energies and the isotropic hyperfine spin coupling constants (hcc) of H_2NO. The hcc's are widely used in electron spin resonance spectroscopy to investigate the structure of radical moieties; they linearly depend on the spin density on the nuclei and can be effectively calculated in condensed phase by a procedure recently developed for the PCM approach,[41] used here for the first time in the COSMO framework.

The solvent induces noticeable geometry rearrangements in this system, in particular that referred to the out-of-plane angle in the bent structure. It is noteworthy that this geometrical change has a negligible effect on the energy of H_2NO in water; nevertheless it heavily affects the value of electronic properties like the isotropic spin coupling constants.

The strong dependence of the calculated quantities on the geometry suggests that vibrational averaging can improve the results sensibly. Following a computational scheme recently applied to other free radicals in solution,[42] we considered a single motion defined as the linear synchronous path joining the minimum and the saddle point; the vibrational coordinate is defined as the arc length along this path in mass-weighted Cartesian coordinates. The hcc's for a number of structures along this path were calculated at the UB3LYP/6-311G(d,p) level and averaged over the first 10 vibrational states at 298 K by the program DiNa;[43] the results are shown in Table 8.

A last comment is in order about the CPU times required by COSMO energy and gradient calculations, compared to the corresponding timings for isolated molecules. As shown in Figure 4a, the time needed for a SCF calculation is about 30% longer in solution than in vacuo for small solutes and only ∼15% longer in the case of larger systems. Notice that both in solution and in vacuo the SCF calculations used the same initial guess (i.e., an INDO wave function, according to GAUSSIAN94 default options); starting from the wave function converged in vacuo, the SCF procedure in solution is even faster. On the

other hand, the calculation of the energy gradients in solution requires less than twice the time needed for isolated molecules; for large solutes, the calculation in solution is only ∼25% longer than that in vacuo (see Figure 4b).

5. Conclusions

We have presented a new implementation of an effective and reliable conductor-like continuum solvation model. Both energy and gradient calculations can be performed at the HF and DF levels; with a suitable choice of cavity sizes, a remarkably good agreement between calculated and experimental solvation energies can be obtained. Many examples show that the possibility to reoptimize molecular geometries taking the solvent effect into account sensibly improves the quality of the description of energies and electronic properties of systems in solution.

The model will be soon extended by including the analytical calculation of energy second derivatives, which presently can be computed by numerical procedures. The limited computational weight required by the calculation of the solvent contributions to energies and gradients makes it possible to apply this procedure also to large systems.

Acknowledgment. This work was supported by the Italian Consiglio Nazionale delle Ricerche.

References and Notes

(1) Tomasi, J.; Persico, M. *Chem. Rev.* **1994**, *94*, 2027.
(2) Rivail, J. L.; Rinaldi, D. Liquid state quantum chemistry. In *Computational chemistry: review of current trends*; Leszcynski, J., Ed.; World Scientific, Singapore, 1995.
(3) Cramer, C. J.; Truhlar, D. G. Continuum solvation models. In *Solvent effects and chemical reactivity*; Tapia, O., Bertran, J., Eds.; Kluwer: Dordrecht, 1996.
(4) Orozco, M.; Alhambra, C.; Barril, X.; Lopez, J. M.; Busquets, M. A.; Luque, F. J. *J. Mol. Model.* **1996**, *2*, 1.
(5) Miertuš, S.; Scrocco, E.; Tomasi, J. *Chem. Phys.* **1981**, *55*, 117.
(6) Cammi, R.; Tomasi, J. *J. Chem. Phys.* **1994**, *100*, 7495.
(7) Foresman, J. B.; Keith, T. A.; Wiberg, K. B.; Snoonian, J.; Frisch, M. J. *J. Phys. Chem.* **1996**, *100*, 16098.
(8) Dillet, V.; Rinaldi, D.; Rivail, J. L. *J. Phys. Chem.* **1994**, *98*, 5034.
(9) Dillet, V.; Rinaldi, D.; Bertran, J.; Rivail, J. L. *J. Chem. Phys.* **1996**, *104*, 9437.
(10) Klamt, A.; Schüürmann, G. *J. Chem. Soc., Perkins Trans. 2* **1993**, 799.
(11) Andzelm, J.; Kölmel, C.; Klamt, A. *J. Chem. Phys.* **1995**, *103*, 9312.
(12) Truong, T. N.; Stefanovich, E. V. *Chem. Phys. Lett.* **1995**, *240*, 253.
(13) Mikkelsen, K. V.; Jorgensen, P.; Jensen, H. J. Aa. *J. Chem. Phys.* **1994**, *100*, 6597.
(14) Mikkelsen, K. V.; Luo, Y.; Ågren, H.; Jorgensen, P. *J. Chem. Phys.* **1994**, *100*, 8240.
(15) Karlström, G. *J. Phys. Chem.* **1989**, *93*, 4952.
(16) Frisch, M. J.; Trucks, G. W.; Schlegel, H. B.; Gill, P. M. W.; Johnson, B. G.; Robb, M. A.; Cheeseman, J. R.; Keith, T.; Petersson, G. A.; Montgomery, J. A.; Raghavachari, K.; Al-Laham, M. A.; Zakrzewski, V. G.; Ortiz, J. V.; Foresman, J. B.; Peng, C. Y.; Ayala, P. Y.; Chen, W.; Wong, M. W.; Andres, J. L.; Replogle, E. S.; Gomperts, R.; Martin, R. L.; Fox, D. J.; Binkley, J. S.; Defrees, D. J.; Baker, J.; Stewart, J. P.; Head-Gordon, M.; Gonzalez, C.; Pople, J. A. *Gaussian 94, Revision B.3*; Gaussian, Inc.: Pittsburgh, PA, 1995.
(17) Stefanovich, E. V.; Truong, T. N. *Chem. Phys. Lett.* **1995**, *244*, 65.
(18) Cossi, M.; Mennucci, B.; Cammi, R. *J. Comput. Chem.* **1996**, *17*, 57.
(19) Pascual-Ahuir, J. L.; Silla, E. *J. Comput. Chem.* **1990**, *11*, 1047.
(20) Silla, E.; Tuñón, I.; Pascual-Ahuir, J. L. *J. Comput. Chem.* **1991**, *12*, 1077.
(21) Pascual-Ahuir, J. L.; Silla, E.; Tuñón, I. *J. Comput. Chem.* **1994**, *15*, 1127.
(22) Cammi, R.; Cossi, M.; Mennucci, B.; Pomelli, C. S.; Tomasi, J. *Int. J. Quantum Chem.* **1996**, *60*, 1165.
(23) Pomelli, C. S.; Tomasi, J. To be published.
(24) Cammi, R.; Tomasi, J. *J. Comput. Chem.* **1995**, *16*, 1449.
(25) Cossi, M.; Barone, V.; Cammi, R.; Tomasi, J. *Chem. Phys. Lett.* **1996**, *255*, 327.
(26) Mennucci, B.; Tomasi, J. *J. Chem. Phys.* **1997**, *106*, 5151.
(27) Klamt, A.; Jonas, V. *J. Chem. Phys.* **1996**, *105*, 9972.
(28) Pierotti, R. A. *Chem. Rev. 76*, **1976**, *76*, 717.
(29) Floris, F. M.; Tomasi, J. *J. Comput. Chem.* **1986**, *10*, 616.
(30) Floris, F. M.; Tomasi, J.; Pascual-Ahuir, J. L. *J. Comput. Chem.* **1991**, *12*, 784.
(31) Caillet, J.; Claverie, P. *Acta Crystallogr.* **1978**, *B34*, 3266.
(32) Cossi, M.; Tomasi, J.; Cammi, R. *Int. J. Quantum Chem., Quantum Chem. Symp.* **1995**, *29*, 695.
(33) Truong, T. N.; Stefanovich, E. V. *J. Chem. Phys.* **1995**, *103*, 3709.
(34) Becke, A. D. *Phys. Rev. B* **1988**, *38*, 3098.
(35) Lee, C.; Yang, W.; Parr, R. G. *Phys. Rev. B* **1988**, *37*, 785.
(36) Barone, V.; Cossi, M.; Tomasi, J. *J. Chem. Phys.* **1997**, *107*, 3210.
(37) Wiberg. K. B.; Laidig, K. E. *J. Am. Chem. Soc.* **1987**, *109*, 5935.
(38) Olivares del Valle, F. J.; Tomasi, J. *Chem. Phys.* **1991**, *150*, 139.
(39) *Handbook of chemistry and physics*; Weast, R. C., Ed.; CRC Press: Cleveland, 1981.
(40) Bondi, A. *J. Phys. Chem.* **1964**, *68*, 441.
(41) Rega, N.; Cossi, M.; Barone, V. *J. Chem. Phys.* **1996**, *105*, 11060.
(42) Rega, N.; Cossi, M.; Barone, V. *J. Am. Chem. Soc.* **1997**, *119*, 12962.
(43) Minichino, C.; Barone, V. *J. Chem. Phys.* **1994**, *100*, 3717. Barone, V.; Minichino, C. *THEOCHEM* **1995**, *330*, 365.